Rev.Adv.Mater.Sci. 23(2010) 133-140

EPR STUDY OF Cr_2Te_3 ALLOY

I. Stefaniuk, M. Bester and M. Kuzma

Institute of Physics, Uniwersity of Rzeszow, ul. Rejtana 16a 35-959 Rzeszów, Poland

Received: December 10, 2009

Abstract. Cr_2Te_3 bulk samples were obtained by melting powdered Cr_2Te_3 at high temperatures (1300-1340 °C). Electron paramagnetic resonance experiments were carried out in an X-band (9.4 GHz) spectrometer in the 150–300K temperature range. There was a great difference between the EPR results of the bulk alloy samples and those obtained for the parent compound, powdered Cr_2Te_3. The transition to the ferromagnetic phase was determined at 212K. Another temperature value of a magnetic phase transition was observed near the room temperature, as well.

1. INTRODUCTION

Chromium chalcogenides may be materials for producing spintronic devices used alternatively to diluted magnetic semiconductors. Cr-chalcogenides reveal a hexagonal crystal structure of the AsNi - type (Fig. 1). Crystals of this type have attracted considerable attention due to their layered structure that determines peculiar electrical and magnetic properties of such materials (e.g. a new FeAs type of high temperature superconductivity [1,2]). Moreover, the variation of the number or arrangement of Cr–vacancies as well as the substitution of metal ions in Cr-chalcogenides lead to the rise of different classes of crystals of the Cr_{1-x}(Te, S, Se) type with a wide range of many fascinating electrical and magnetic properties which depend on the number of Cr vacancies indicated by x. Crystals of these compounds such as $Cr_{1-x}Te$ [3] exhibit antiferromagnetism, non-collinear spin structures or itinerant electron magnetism [4]. The substitution of Cr atoms with Ti or V creates new properties such as spin-glass [5,6].

Premelted $Cd_{1-x}Te$ for x=0.33 (x determines the number of Cr vacancies) i.e. Cr_2Te_3 are studied in this paper. The structure of this compound belongs to the trigonal system and is presented in Fig. 1. The Cr vacancies lie in every second metal layer and they are ordered in the vacancy layers as can be seen in Fig. 1 [7,8]. The elementary cell (a= 0.6823 nm, c= 0.1180nm [9]) is doubled in respect to the CrTe.The Curie temperature is 170-180K. Theoretical calculations result in the magnetic moment of 3.03 μ_B per Cr, whereas neutron diffraction measurements predict ferromagnetic moments of 2.6 μ_B for Cr atoms situated in fully occupied layers and it is almost negligible for Cr in vacancy layers [9].

Chromium tellurides are mainly ferromagnetic with metallic conductivity (e.g. CrTe is a metal with T_c = 340K). Chromium antimonides, on the contrary, are metallic antiferromagnets with ferromagnetic planes perpendicular to the c axis (T_N = 710K). Chromium sulphides are antiferromagnetic semiconductors like selenides, but the latter reveal metallic conductivity.

Some chalcogenides (such as $Cr_{1-x}Te$ or $Cr_{1-x}Se$) exhibit a metastable zinc-blende structure [10] which allows for growth of the zinc-blende solid solution semiconductor compounds with the proper-

Corresponding author: M. Kuzma, e-mail: kuzma@univ.rzeszow.pl

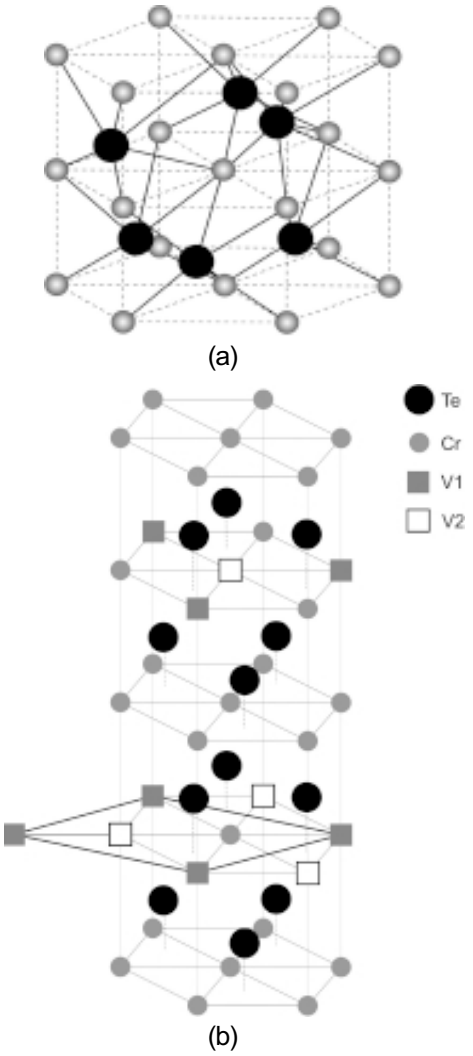

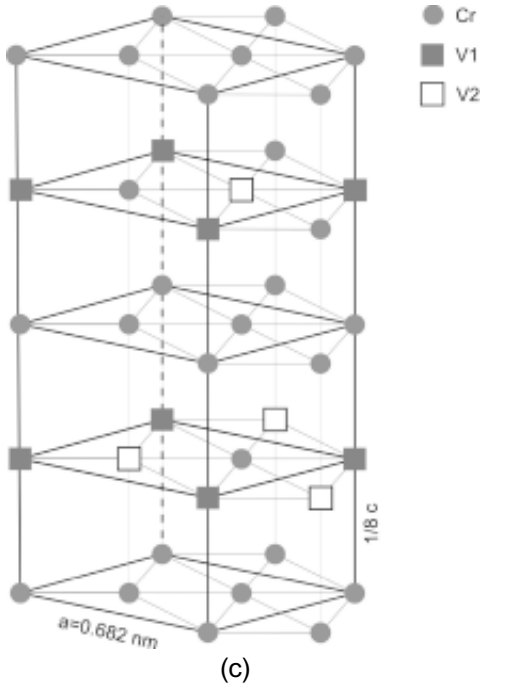

Fig. 1. Crystal structure of AsNi (a) and of Cr_2Te_3 (b). Elementary cell of Cr_2Te_3 (c), (square symbols denote Cr vacancies).

ties of diluted magnetic semiconductors, e.g., CrMnTe [11], ZnCrTe [12], ZnCrSe [13]. Recently, Ko and Blamire [14,15] have reported room-temperature ferromagnetism in CrCdTe crystals. In our investigations we have also observed this phenomenon [16]. The origin of such ferromagnetism is not clearly understood yet, and the assumption that it may follow from the $Cr_{1-x}Te$ precipitates motivates the aim of the present paper to study the magnetic resonance properties of this compound.

2. EXPERIMENTAL

A CrTe alloy was prepared by melting powdered Cr_2Te_3 (Alfa Aesar, 99.5%) in an evacuated quartz ampoule at the temperatures of 1300, 1320, and 1340 °C. These particular melting temperatures were chosen because such temperatures were considerably higher than those used in the interdiffusion method of the synthesis of various phases of the Cr-Te system which were in the range of 1100 – 1200 °C [17]. Those higher temperatures seemed to be more advantageous in the synthesis of the three component solid solutions obtained from the melt, based on Cr-chalcogenides and, e.g., Cd-chalcogenides CdTe-CrTe. The melting temperatures proposed by us did not lead to a decomposition of the materials but facilitated homogeneity of the final product. The times of heating and cooling are listed in Table 1. The ingots show a porosity, brittle structure consisting of fine grains. The structure of the samples was examined with optical and scanning electron microscopy.

The EPR spectra were recorded using an X-band (9.4 GHz) spectrometer provided with a gas nitrogen cryostat (Oxford Instrument) with a nominally stabilizing temperature of the sample in the range of 77–500K. The measurements were taken in the temperature range of 150-350K.

Table 1. The $Cr_{1-x}Te$ alloy samples prepared for this study.

sample	crystal	melting temp. [°C]	melting time	cooling time
1	$Cr_{1-x}Te$	1300	1 h	3 h 15 min
2	$Cr_{1-x}Te$	1320	1 h	3 h 45 min
3	$Cr_{1-x}Te$	1340	30 min	4 h
4	Cr_2Te_3 powder	-	-	-

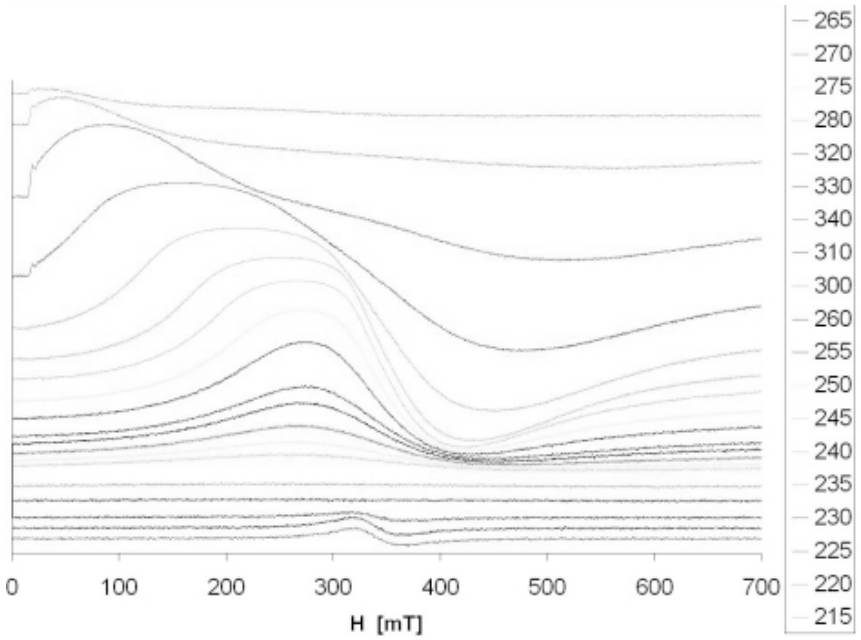

Fig. 2. EPR spectra of Cr_2Te_3 (sample No.1) at different temperatures.

3. RESULTS AND DISCUSSION

The temperature dependence of the EPR spectrum of sample No. 1 is shown in Fig. 2.

As can be seen in Fig. 2, the shape of the EPR line depends strongly on the temperature. In the vicinity of the room temperature the lines become very broad and weak or disappear completely. At lower temperatures the shape of the lines approaches the Lorentz function. The asymmetry of the lines is also visible which can be attributed to the strong exchange interactions as well as to the semimetal electrical conductivity. The shape of the spectra is characteristic for a paramagnetic phase above room temperature.

We extracted the parameters of the lines: intensity I, resonance field H_r and width H_{pp} from the fitting of the theoretical Lorentz formulae to the experimental spectra at each temperature. Many lines were shifted significantly to the small resonance fields which resulted in partial detection of the resonance signal derivative. In such case it was possible to fit the recorded part of the line with the Lorentz behaviour as well. In Fig. 3 the fits of the experimental EPR line to the Lorentz function are presented as an example.

Fig. 4 shows the linewidth and the g factor dependence on temperature for samples Nos. 1, 2, and 3. Above room temperature the lines are stable with regard to both their position and width, and they are relatively narrow. Two temperature ranges can be seen in Fig. 4 where the linewidth increases drastically and the line disappears absolutely. This takes place for the temperature range of 280–300K and below 220K.

The calculated g factor at the room temperature has the value of 1.98. The factor changes moder-

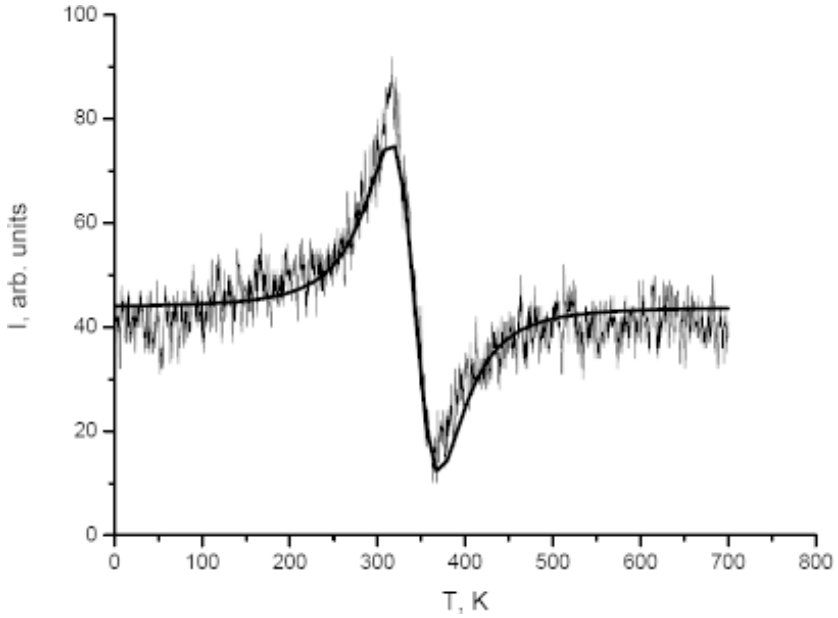

Fig. 3. Fits of the experimental EPR line to the Lorentz function (sample No. 3, T =320 °C).

ately below the room temperature due to the rise of an internal field. This change is however quite significant below 220K.

In Fig. 5. we have compared the spectra of Cr_2Te_3 alloys (samples Nos. 1, 2, 3) with those obtained for the powdered Cr_2Te_3 (sample No. 4) which was the parent material for the preparation of alloy samples. These spectra were recorded at room temperature. As can be observed, there is a great difference between the spectra of the latter sample and those of the former ones.

Comparing the EPR spectra for samples Nos. 1, 2, 3 it can be concluded that the technological parameters applied in the present study influence strongly neither the EPR spectrum line width nor the discontinuity position of temperature dependencies in the diagrams. However, there is a strong dependency of the line position (g factor) on the melting temperature. The difference is especially visible for EPR measurements at low temperatures (see Fig. 4b).

The EPR spectra of sample No 2 exhibit non-ordinary features. Below 290K, the spectra consist of two lines as can be seen in Fig. 6. The dominated line moves towards low magnetic resonance fields with the decreasing temperature, whereas the second line is going in the opposite direction. Both components are relatively wide, and the second line is of a much smaller intensity. The large broadening of the investigated lines is a result of the great interaction between magnetic moments. On the other hand, the EPR line splitting into two components in the case of sample No. 2 at lower temperatures can be attributed to a great magnetic anisotropy in the ferromagnetic phase. The samples reveal a crystal structure with a prevailing axial symmetry [10], giving two g factor values: $g_{\|}$ and $g_{\perp}$. In polycrystalline samples, all spins are statistically randomly oriented. Therefore, it may be expected to observe the EPR spectrum spreading over the ΔB field range determined by the g tensor. However, the lines are not uniformly distributed over this magnetic field range. Thus, the great magnetic anisotropy for polycrystalline samples results in the rise of two lines in the EPR experiment [18]. The effect is enhanced considerably in the ferromagnetic state. The temperature dependence of the positions of these two lines of sample 2 is presented in Fig. 7 as a shift $H_r(T) - H_r(240\text{K})$ of the line positioning from the high temperature limit $H_r(240\text{K})$. Such behavior is intrinsic to the layered magnetic systems with two-dimensional ferromagnetic fluctuations above the Curie temperatures. It has been also observed in layered perovskite manganites (see e.g. [19]).

The inset in Fig. 4a shows the least-square fit of Huber's [20] expression: to a part of the $\Delta H_{pp}(T)$ data

$$\Delta H_{pp} = A\left(\frac{T_c}{T - T_c}\right)^a + B, \qquad (1)$$

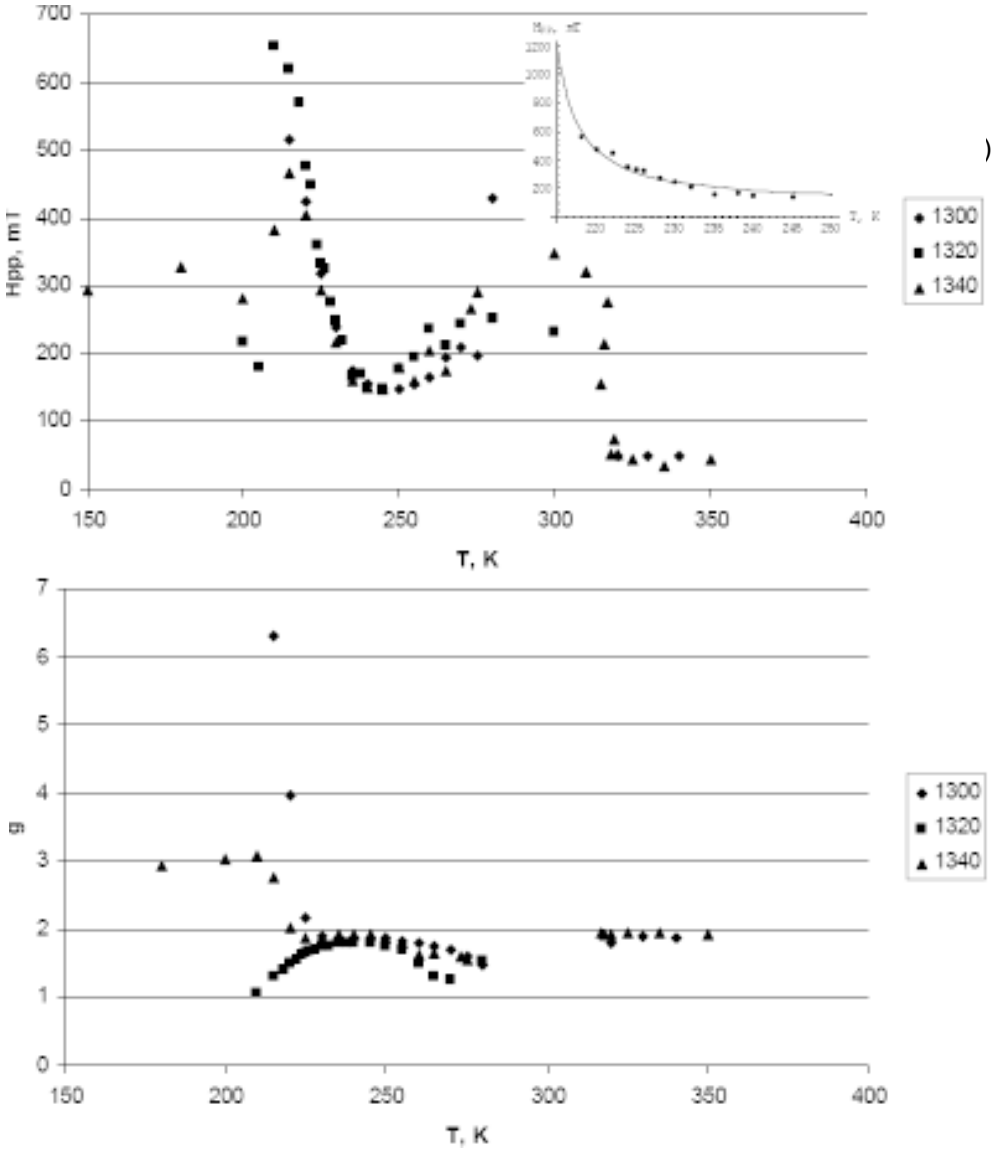

Fig. 4. Dependencies of the linewidth (a) and the g factor (b) on temperature for samples 1 (1300), 2 (1320), and 3 (1340).

where α is a critical exponent, B is the temperature-independent linewidth, T_C is the order-disorder transition temperature, A is a constant.

The value of T_C determined from Eq. (1) is found to be T_C = 212K at α = 1.1 and B = 95 mT. This value is identified with the Curie temperature as the α is close to the value of 1. Thus, the Huber's equation approximates the Curie –Weiss law. So far, a number of $Cr_{1-x}Te$ compounds have T_C ranging from 170K to 360K depending on the number x of Cr vacancies (Table 2). The value of T_C obtained in our paper does not match any of those listed in Table 2, even this for the parent compound Cr_2Te_3. The difference could be due to the clustering of chromium atoms in the layers, which results in a decrease in x and enhanced T_C.

In Fig. 8 we have collected the integrated intensity I_{EPR} for all the three samples calculated as:

$$I_{EPR} = I\left(\Delta H_{pp}\right)^2, \qquad (2)$$

where I is the amplitude of the EPR absorption field derivative.

The anomaly in the temperature dependence of the EPR linewidth and the integrated intensity observed at room temperature in Fig. 4 and in Fig. 8 could be attributed to low–dimensional ferromagnetic effects. Such low–dimensional ferromagnetic fluc-

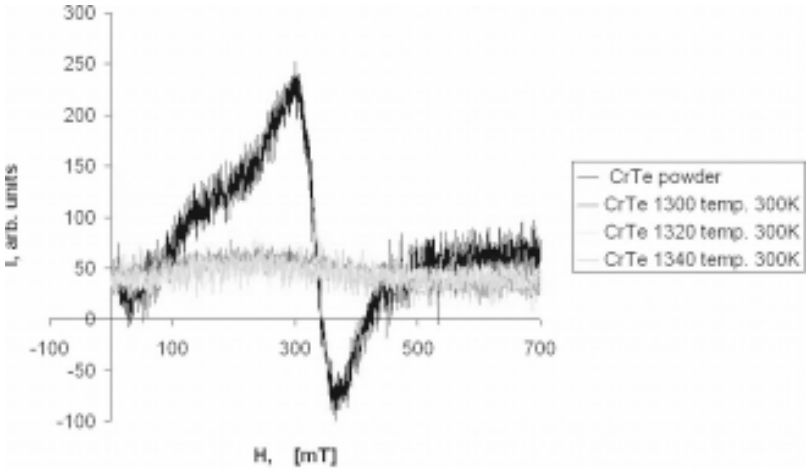

Fig. 5. EPR spectra for powdered Cr_2Te_3 (sample No 4) and melted Cr_2Te_3.

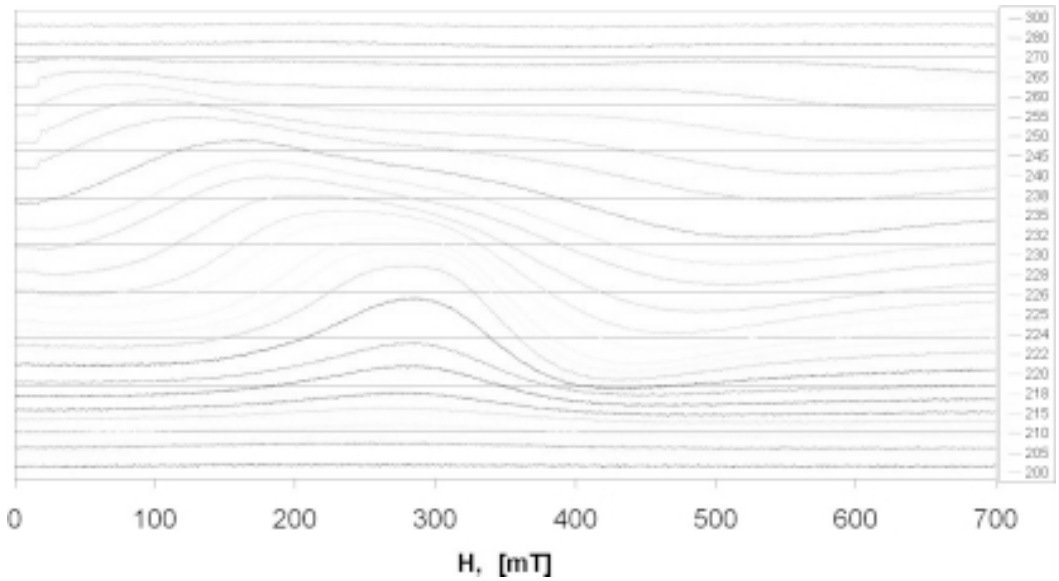

Fig. 6. EPR spectra for sample No2.

tuations may follow a high-temperature magnetic transition. Chauvet *et al.* [24] observed the magnetic transition at 350K above the Curie temperature T_c= 110K in the layered manganites $La_{1.35}Sr_{1.65}Mn_2O_7$. Moreno et al. [19] investigated also manganites $La_{1.35}Sr_{1.65}Mn_2O_7$ and $La_{1.2}Sr_{1.8}Mn_2O_7$ by EPR and observed additional transitions for T~ 450-500K also well above T_c. The linewidth anisotropy and the spectrum splitting into two lines with the decreasing temperature were addressed as intrinsic features of the layer systems. Recently, two-dimensional spin fluctuations in layer crystals GdI_2 have been studied by EPR by Deisenhofer [25]. The experimental results have been described by a two-dimensional Heisenberg ferromagnet model proposed by Eremin et al. [26]. The structure of GdI_2 is similar to that of chromium chalcogenides. There are hexagonal planes of magnetic ions. These planes are separated by planes of nonmagnetic I ions. The high-temperature two-dimensional ferromagnetic transition in GdI_2 was observed at T_c = 276K [25].

In Fig.8 the theoretical dependence $\chi(T)$ given by Deisenhofer [25] has been plotted (as a solid line):

$$\chi_{spin}(T) \propto \left(\exp\left(-\frac{16\sqrt{3}S^2 J_{\|}}{T} \right) - \frac{J_{\perp}}{6\sqrt{3}SJ_{\|}} \right)^{-1} \quad (3)$$

for S=3/2, $J_{\|}$= 57, $J_{\perp}$=0.006, and A =1.4*10^{-6}.

Here $J_{\|}$ and $J_{\perp}$ are ferromagnetic exchange constants within and inter the Cr layers, respectively, A

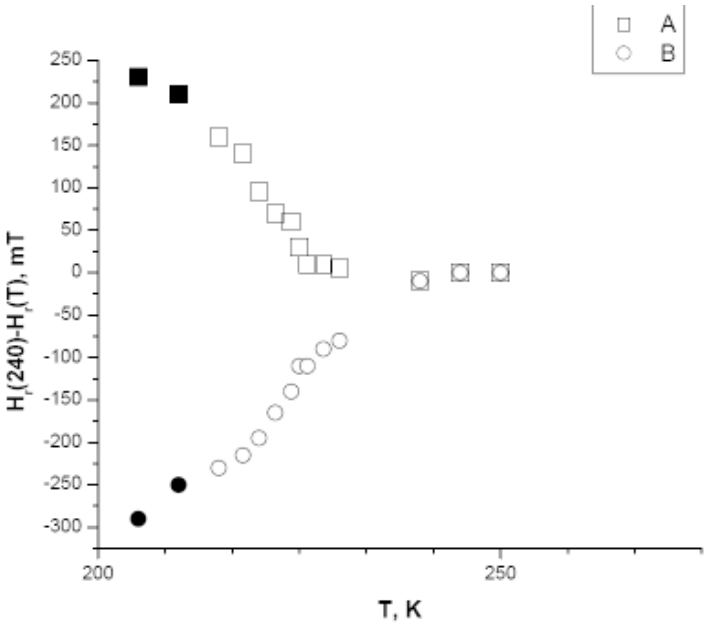

Fig. 7. The resonance shift dependence of two lines of samples No. 2 (In Fig. 4. only the line at a weak magnetic field is taken into account. The solid signs denote measurements with a great error bar).

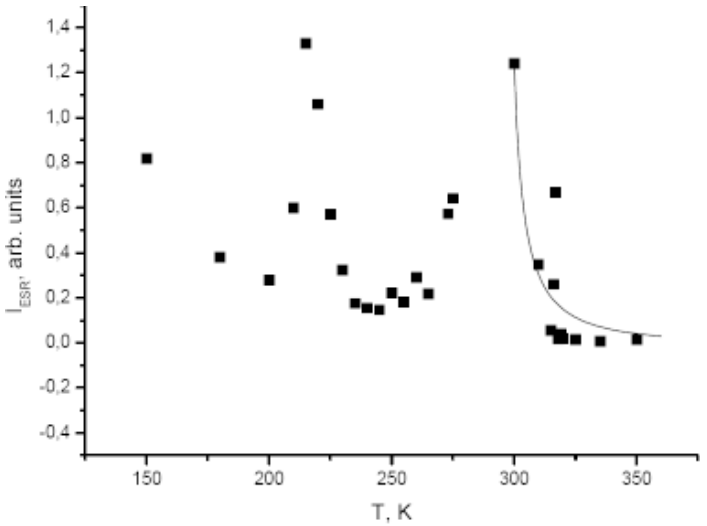

Fig. 8. Integrated intensity of samples No. 1, 2, 3.

Table 2. Curie temperatures for $Cr_{1-x}Te$ compounds.

$Cr_{1-x}Te$	CrTe	$Cr_{23}Te_{24}$	Cr_7Te_8	Cr_5Te_6	Cr_3Te_4	Cr_2Te_3
x	0	0.042	0.125	0.167	0.25 [4]	0.33
T_c	328K [17] 343K [21] 342K [22] 350K [23]	327K [17]	326K [17]	320K [17]	317K [17] 340K [8]	170- 180K [8]

is the proportionality coefficient. It can be noticed that the agreement of the theoretical dependence with the experimental data, particularly in a high temperature regime, is not very good. Nevertheless, these dependence estimates adequately the Curie temperature of the two-dimensional ferromagnetic fluctuations addressed by us. However, at this stage of the study the supposition that this high-T mag-

netic transition is not intrinsic for our layer system but follows from the second phase cannot be rigorously rejected. Such discrepancies in the interpretation of the data exist in literature (see e.g. Moreno et al. [19] and the references therein).

4. CONCLUSIONS

The crystal structure of Cr_2Te_3 gives grounds to assert that the magnetism in the plane perpendicular to *c* axis is two-dimensional. The *g* factor and the linewidth dependence on temperature indicates the presence of two temperatures at which magnetic transitions are observed. The first transition, around 300K, can be assumed to be a result of two-dimensional ferromagnetic correlated Cr clusters in the *a-b* plane. The second transition, at 212K, is attributed to the phase transition of bulk ferromagnetism. The measurements of sample 2 (heating temperature 1320 °C) show the presence of strong magnetic anisotropic effects resulting in the EPR line splitting above the Curie temperature.

REFERENCES

[1] Y. Kamihara, T. Watanabe, M. Hirano and H. Hosono // *J. Am. Chem. Soc.* **130** (2008) 3296.
[2] X. Huang, *arXiv:0805.0355v1 [cond-mat.str-el]* 3 May 2008.
[3] G. Chattopadhyay // *J. of Phase Equlibria and Diffusion* **15** (1994) 1547.
[4] K. Shimada, T. Saitoh, A. Fujimori, S. Ishida, S. Asano, M. Matoba and S. Anzai // *Phys. Rev. B* **53** (1996) 7673.
[5] S. Ohta // *J. Phys. Soc. Jpn.* **54** (1985) 1076.
[6] G. Makovetskii and S. Dorofeichik // *Inorganic Materials* **43** (2007) 591.
[7] H. Ipser, K.I. Komarek and K.O. Klepp // *J. Less. Common Met* **92** (1983) 265.
[8] J. Dijkstra, H.H. Weitering, C.F. van Bruggen, C. Hass and R.A. deGroot // *J. Phys.: Condens. Matter* **1** (1989) 9141.
[9] T. Hamasaki, T. Hashimoto, Y. Yamaguchi and H. Watanabe // *Solid State Commun.* **16** (1975) 895.
[10] J.F. Bi, M.G. Sreenivaxan, K.L. Teo and T.J. Liew // *J. Pys. D: Appl.Phys.* **41** (2008) 045002.
[11] K. Nakamura, A.J. Freeman and T. Ito // *Phys. Rev. B* **72** (2005) 064449.
[12] L. Zhao, B. Zhang, Q. Pang, S. Yang, X. Zhang, W. Ge and J. Wang // *Apl. Phys. Lett.* **89** (2006) 092111.
[13] W. Mac, N. The Koi, A. Twardowski, J.A. Gaj and W. Demianiuk // *Phys. Rev. Lett.* **71** (1993) 2327.
[14] K.Y. Ko and M.G. Blamire // *Apl. Phys. Lett.* **88** (2006) 172101.
[15] K.Y. Ko and M.G. Blamire // *J. of Korean Phys. Soc.* **49** (2006) 591.
[16] I. Stefaniuk, M. Bester and M. Kuzma // *J. Phys.: Conf. Ser.* **104** (2008) 012010.
[17] M. Akram and F.M. Nazar // *Journal of Materials Science* **18** (1983) 423.
[18] J.A. Weil, J.R. Bolton and J.E. Wertz // *Electron Paramagnetic Resonance, Elementary Theory and Prctical Applications* (A Wiley-Interscience Publication, New York, 1994).
[19] N.O. Moreno, P.G. Pagliuso and C. Rettori // *Phys. Rev. B* **63** (2001) 174413-1.
[20] D.L. Huber // P*hys. Rev. B* **6** (1972) 3180.
[21] N. Suzuki, T. Kanomata, R. Konno, T. Kaneko, H. Yamauchi, K. Koyama, H. Nojiri, Y. Yamaguchi and M. Motokawa // *Journal of Alloys and Compounds* 290 (1999) 25.
[22] N.P. Grazhdankina and R.I. Zinullina // *Sov. Phys. JETP* **32** (1971) 1025.
[23] S. Ohta, T. Kanomata, T. Kaneko and H. Yoshida // *J. Phys.: Condens. Matter* **5** (1993) 2759.
[24] O. Chauvet, G. Goglio, P. Molinie, B. Corraze and L. Brohan // *Phys. Rev. Lett.* **81** (1998) 1102.
[25] J. Deisenhofer, Krug von Nida and A. Loidl, *arXiv:cond –mat/0401415v1,* 2004.
[26] I. Eremin, P. Thalmeier, P. Fulde, R.K. Kremer, K. Ahn and A. Simon // *Phys. Rev. B* **64**(2001) 064425-1.